Biomaterials 268 (2021) 120606

Contents lists available at ScienceDirect

Biomaterials

journal homepage: www.elsevier.com/locate/biomaterials

An urchin-like helical polypeptide-asparaginase conjugate with mitigated immunogenicity

Yali Hu [a,c], Dedao Wang [b], Hao Wang [a], Ruichi Zhao [a], Yaoyi Wang [a], Yunfei Shi [d], Jun Zhu [b], Yan Xie [b,**], Yu-Qin Song [b,***], Hua Lu [a,*]

[a] Beijing National Laboratory for Molecular Sciences, Center for Soft Matter Science and Engineering, Key Laboratory of Polymer Chemistry and Physics of Ministry of Education, College of Chemistry and Molecular Engineering, Peking University, Beijing, 100871, People's Republic of China
[b] Key Laboratory of Carcinogenesis and Translational Research (Ministry of Education), Department of Lymphoma, Peking University Cancer Hospital & Institute, 52 Fucheng Road, Haidian District, Beijing, 100142, People's Republic of China
[c] Peking-Tsinghua Center for Life Sciences, Academy for Advanced Interdisciplinary Studies, Peking University, Beijing, 100871, People's Republic of China
[d] Key Laboratory of Carcinogenesis and Translational Research (Ministry of Education), Department of Pathology, Peking University Cancer Hospital & Institute, 52 Fucheng Road, Haidian District, Beijing, 100142, People's Republic of China

A B S T R A C T

The use of asparaginase (ASNase), a first line drug for lymphoma treatment, is impaired by short circulation and notoriously high immunogenicity. Although PEGylation can prolong the circulating half-life of ASNase, however, it also induces anti-PEG antibodies that lead to accelerated blood clearance (ABC) and hypersensitivity reactions. Here, we create an urchin-like polypeptide-ASNase conjugate P(CB-EG$_3$Glu)-ASNase, in which the surface of ASNase is sufficiently shielded by an array of zwitterionic helical polypeptides through the labeling of the ε-amine of lysine. The conjugate is fully characterized with size exclusion chromatography, SDS-PAGE, dynamic light scattering, and circular dichroism. *In vitro*, P(CB-EG$_3$Glu)-ASNase retains full activity based on the enzymatic assay using the Nessler's reagent and cell viability assay. *In vivo*, examination of the enzyme activity in serum indicates that P(CB-EG$_3$Glu)-ASNase prolongs the circulating half-life of ASNase for ~20 fold. Moreover, P(CB-EG$_3$Glu)-ASNase significantly inhibits tumor growth in a xenografted mouse model using human NKYS cells. Importantly, P(CB-EG$_3$Glu)-ASNase elicits almost no antidrug or antipolymer antibodies without inducing ABC effect, which is in sharp contrast with a similarly produced PEG-ASNase conjugate that develops both antidrug/antipolymer antibodies and profound ABC phenomenon. Our results demonstrate that urchin-like conjugates are outstanding candidates for reducing immunogenicity of therapeutic proteins, and P(CB-EG$_3$Glu)-ASNase holds great promises for the treatment of various lymphoma diseases.

1. Introduction

Lymphoma, caused by malignant transformation of lymphoid cells, is a family of cancers with many subtypes including acute lymphocytic leukemia (ALL), lymphoblastic lymphoma (LBL), and NK/T cell lymphoma [1]. Among them, NK/T cell lymphoma is a relatively aggressive subtype and naturally resistant to anthracyclines such as doxorubicin due to the high expression of P-glycoprotein (P-gp) [2]. The implement of L-Asparaginase II (ASNase), now a first-line drug for NK/T cell lymphoma treatment, improves the five-year overall survival rate from ~31% for anthracycline-containing regimens to ~55% [3]. By depleting external circulating L-asparagine (Asn), the tetramer of ASNase induces the apoptosis of tumor cells that cannot make their own Asn, while normal cells are less affected [4]. As a notoriously high immunogenic protein originated from bacteria such as *E. coli.* or *Erwinia*, however, ASNase is well known to evoke hypersensitivity and/or allergic (HA) reactions of patients. According to previous clinical studies, ~20–30% patients developed HA reactions to ASNase, with approximately half of those defined as severe [5,6]. To tackle these clinical challenges, a PEGylated *E. coli.* ASNase, under the trade name of Oncaspar®, has been developed to shield the antigenic epitopes and prolong the *in vivo* acting lifetime of ASNase [7]. In a recent retrospective analysis, the so-called SMILE regimen with Oncaspar® as one of the major components resulted in a 80% complete response rate, significantly higher than the 30% of conventional CHOP-like regimen (combination of cyclophosphamide, doxorubicin, vincristine, and prednisone) [8]. The global sale of Oncaspar® reached 205 million USD in 2019 and is projected to climb to 320 million by 2025.

* Corresponding author.;
** Corresponding author.
*** Corresponding author.
E-mail addresses: xieyan9@263.net (Y. Xie), songyuqin622@163.com (Y.-Q. Song), chemhualu@pku.edu.cn (H. Lu).

https://doi.org/10.1016/j.biomaterials.2020.120606
Received 29 August 2020; Received in revised form 9 December 2020; Accepted 12 December 2020
Available online 17 December 2020

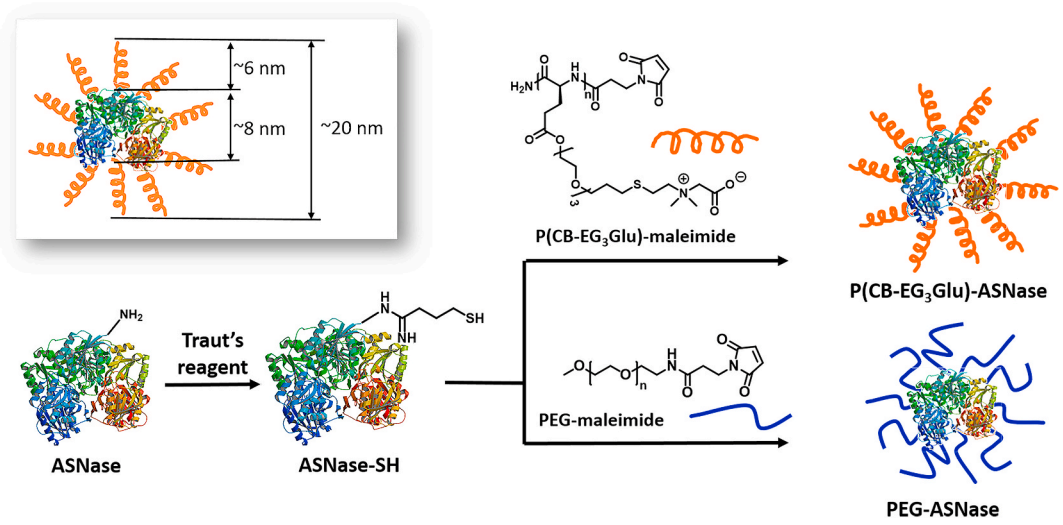

Scheme 1. Synthesis of the two polymer-ASNase conjugates, P(CB-EG_3Glu)-ASNase and PEG-ASNase. Structural cartoon of the ASNase tetramer was adapted from PDB ID 3ECA [41].

Despite the effectiveness of PEGylation, there were still 12.8% patients (79/615) developed HA to the treatment of Oncaspar® [9]. In another clinical study, nearly half the Oncaspar® treated patients (13/28) were tested positive for anti-PEG antibodies in the sera, and a strong correlation was established between the occurrence of anti-PEG IgM and the rapid drug clearance (undetectable ASNase activity), known as the accelerated blood clearance (ABC) [10]. In a recent phase 2 clinical trial, a recombinant PEGylated *Erwinia* asparaginase was shown to induce hypersensitivity reactions and rapid clearance of serum ASNase activity in 75% (3/4) pediatric patients due to the presence of anti-PEG antibodies [11].

To circumvent the limitations of PEG [12–17], a number of recombinant or synthetic polymers have been proposed as alternatives to PEG including XTEN [18], PAS [19], ELP [20], polyglycerol [21,22], poly (2-oxazoline)s [23], zwitterionic polymers [24–28], polysulfoxide [29], poly(2-hydroxypropyl methacrylate) (PHPMA) [30], polypeptides [31,32], and poly(*N*-acryloylmorpholine) [33]. For instance, Gauthier and coworkers exploited a cylinder-like comb polymer pOEGMA, that is OEGylated poly(methacrylate), for ASNase modification, which outperformed a mPEG-ASNase conjugate in terms of reduced immune response [34]. However, the study reported considerable *in vitro* activity loss of ASNase without *in vivo* antitumor efficacy disclosed. Moreover, as pointed out by Chilkoti, the antigenicity of pOEGMA is dependent on the length of the side chain OEG, and a OEG_9 side chain is long enough to induce anti-PEG antibodies [35]. As such, more detailed follow-up studies are necessary to determine whether the ASNase-pOEGMA conjugates (in which the OEG length = 8–10) can avoid the undesired ABC effect upon repeated administration.

In nature, sea urchins use a cluster of rigid spines to protect themselves from predators. Inspired by this, we hypothesize that an urchin-like conjugate (Scheme 1 inset), in which the core protein is protected by an array of rigid spine-like polymers rather than conventional flexible PEG, could be promising for low immunogenicity. The rigidity of antifouling polymer may help form a more repulsive layer preventing the immune system from approaching and attacking. For example, the semipermeability pOEGMA with an extended conformation, when conjugated to ASNase, played a better role in reducing immunogenicity than the flexible PEG did [34]. Some polypeptides are well known adopting α-helical conformation with a rigid rod-like shape. For example, the helical poly(γ-(2-(2-(2-methoxyethoxy)ethoxy)ethoxy)esteryl $_L$-glutamate) ($_L$-P(EG_3Glu)), showed superior surface antifouling performance as relative to PEG [36,37]. This phenomenon was further validated in the context of protein conjugates, in which the site-specific conjugation of $_L$-P(EG_3Glu) to the *N*-terminus of human interferon (IFN) or growth hormone led to profoundly less antidrug antibodies (ADA) generation as compared to PEGylation [38]. However, it remains largely unknown whether such observations can be generally applied to more immunogenic proteins, using different helical polypeptides, and/or with different conjugation sites. For this, we hypothesize that an urchin-like ASNase conjugate randomly attaching multiple rigid helical polypeptides, could maximumly block the immunogenic epitopes of ASNase and thus reduce its immunogenicity *in vivo*. It should be mentioned that, during the review process of this manuscript, Jiang et al. masked the surface of ASNase using a triple-layered EK-peptide cloak for elimination of the immunogenicity [39].

2. Methods

2.1. General protocol for the synthesis of polymer-ASNase conjugates

To ASNase (4.5 mg, 0.12 μmol, 1.0 equiv) in phosphate buffer (pH 8.0) was added 2-iminothiolane hydrochloride (1.0 mg, 7.3 μmol, 60 equiv) in dimethyl sulfoxide (5% V/V). The reaction was incubated at 25 °C for 80 min before removing all the unreacted small molecules by passing through a PD-10 desalting column (GE, USA). The obtained solution was concentrated to 1.0 mL, mixed with the designated maleimide-functionalized polymer (60 equiv), and incubated at 4 °C overnight. SDS-PAGE indicated a complete conversion of ASNase and the free polymer was conveniently removed using ÄKTA with a SEC column (superdex 200 increase 10/300 GL). The afforded pure conjugate was stored in PBS buffer (pH 7.4) at 4 °C and lipopolysaccharide (LPS) was removed before *in vivo* injection by using endotoxin affinity beads (Senhui Microsphere Tech Co., Ltd, China).

2.2. Enzyme activity assay

In vitro enzyme activity was measured by detecting the produced ammonium using Nessler's reagent (Merck, Germany). Briefly, in a transparent 96-well plate, phosphate buffer (90 μL, pH 7.4), sample solution (10 μL), and $_L$-asparagine solution (20 μL, 40 mM) were mixed and reacted at 37 °C for 10 min. The reaction was terminated by trichloroacetic acid solution (TCA, 20 μL, 1.5 M) and centrifuged at 1000 g for 5 min. The supernatant (20 μL) was added to another transparent 96-well plate containing Nessler's reagent (20 μL, Merck, Germany) in phosphate buffer (160 μL, pH 7.4). Absorption at 410 nm were then measured by using a multimode plate reader (PerkinElmer, USA). A

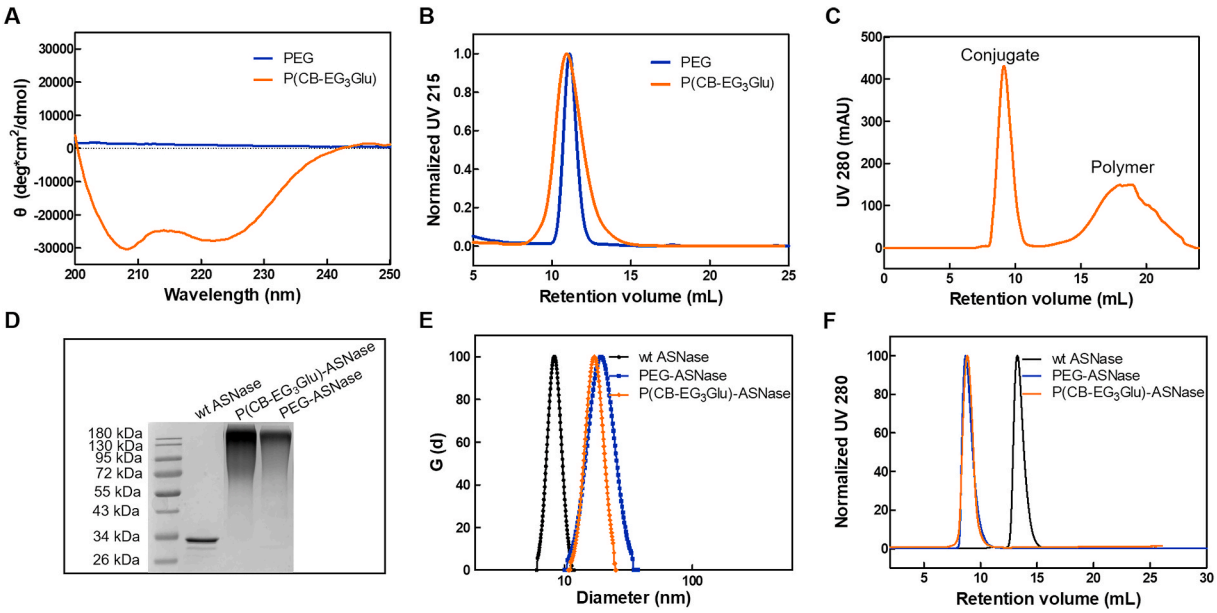

Fig. 1. Characterization of polymers and the corresponding polymer-ASNase conjugates. (A) Circular dichroism (CD) spectroscopy and (B) size exclusion chromatography (SEC) of P(CB-EG_3Glu) and mPEG used for conjugation. (C) A representative SEC trace of the conjugation reaction mixture. (D) SDS-PAGE analysis, (E) dynamic light scattering (DLS), and (F) SEC traces of wt ASNase and the purified polymer-ASNase conjugates.

series of ammonium with known concentrations were used to prepare the standard working curve for the calculation of ASNase concentration. One unit of ASNase is defined as the amount of enzyme required to generate 1.0 μmole ammonia per minute at pH 7.4 and 37 °C.

2.3. Immunization and ELISA

Male and female SD rats were randomly grouped (n = 4) and received wt ASNase, P(CB-EG_3Glu)-ASNase, or PEG-ASNase subcutaneously at a weekly 200 U ASNase/kg dose. Blood were drawn and sera were acquired before the immunization for benchmark (day 0), and one week after each injection (day 7, 14, 28, and 35). The ADA and antipolymer antibodies in the sera were then evaluated by ELISA. For the 5th immunization, sera were collected at pre-determined time points after the i.v. injection for pharmacokinetic evaluation (based on the enzyme activity assay described above).

The antigens used in direct ELISAs: wt ASNase (for the detection of anti-ASNase IgG and IgM), P(CB-EG_3Glu)-IFN conjugate (for the detection of anti-P(CB-EG_3Glu) antibody), and PEG-IFN conjugate (for the detection of anti-PEG antibody). The polypeptide-IFN [40] and PEG-IFN [32] conjugates were made by following the published protocols.

ELISA procedure for antipolymer IgM measurement: Polymer-IFN conjugates in PBS (100 μL × 1.0 μg/mL/well) were added to high-binding transparent 96-well plates (Corning, USA) and incubated at 4 °C overnight for antigen coating. The plate was washed with Wash Buffer (0.5‰ CHAPS in PBS, 200 μL/well × 3), and blocked with Assay Buffer (5% BSA in wash buffer, 100 μL) at room temperature for 2 h before adding the sample solution. Next, prediluted sera (100 μL, 200-fold dilution with the Assay Buffer) were added to the washed plate and incubated at room temperature for 1 h. Subsequently, the plate was washed for three times using Wash Buffer, and incubated with the secondary antibody goat anti-rat IgM mu chain HRP (100 μL, 5000-fold dilution with Assay Buffer) at room temperature for 1 h. Finally, after washing for four times, the plate was incubated with TMB solution (100 μL, CWBIO) at room temperature for the chromogenic reaction. The reaction was terminated 5 min later with 2 N H_2SO_4 (100 μL) before reading the absorption at 450 nm in a plate reader.

ELISA procedure for anti-ASNase IgG/IgM and antipolymer IgG: the procedure was similarly carried out as mentioned above but different in the coating antigens, dilution fold, and buffer recipe. More detailed information were available in Table S1.

2.4. Statistical analysis

Data are presented as means ± standard deviations. Statistical analysis was calculated on GraphPad Prism 5.0, based on one-way or two-way ANOVA using Type III sum-of-squares, and multiplicity of post-tests was controlled by Bonferroni correction. Statistical significance was marked with asterisk (*P < 0.05, **P < 0.01, ***P < 0.001) in the figures, ns = no significant difference.

3. Results and discussion

3.1. Synthesis and characterization

To test the hypothesis mentioned above, we synthesized $_L$-P(CB-EG_3Glu) (M_n = 17 kDa, DP = 40, synthesis and characterization see SI), a helical poly($_L$-glutamate) that bears a short EG_3 linker connecting to a zwitterionic carboxybetaine group in its side chain (Scheme 1 and Fig. 1A) [36,42]. This polymer was previously found exceptional in constructing ultralow fouling surfaces *in vitro*, but was never attempted for protein conjugation nor studied in any *in vivo* experiment. Thus, it would serve as a suitable candidate for ASNase modification. Random and complete labeling of ASNase by excessive polymers were conducted in the current study using thiol-maleimide chemistry in order to afford an urchin-like three dimensional structure (Scheme 1). To do this, the ε-amines of lysine residues of ASNase were converted to thiols by using 2-iminothiolane (Traut's reagent) to afford ASNase-SH. In the meantime, $_L$-P(CB-EG_3Glu) was reacted with *N*-succinimidyl 3-maleimidopropionate to install the maleimide moiety (Scheme S1 and Figure S1-2). The conjugation of maleimide-functionalized $_L$- P(CB-EG_3Glu) to ASNase-SH were carried out under physiological conditions, e.g. pH 8.0 and 4 °C for 12 h, yielding the desired product P(CB-EG_3Glu)-ASNase. A control conjugate PEG-ASNase was synthesized by following the same chemistry using a mPEG of 5 kDa (a molecular weight that was used in Oncaspar®), which showed a similar hydrodynamic size to $_L$-P(CB-EG_3Glu) (Fig. 1B). Complete conversions of ASNase to conjugates were observed in both two reactions, as revealed by SDS-PAGE analysis

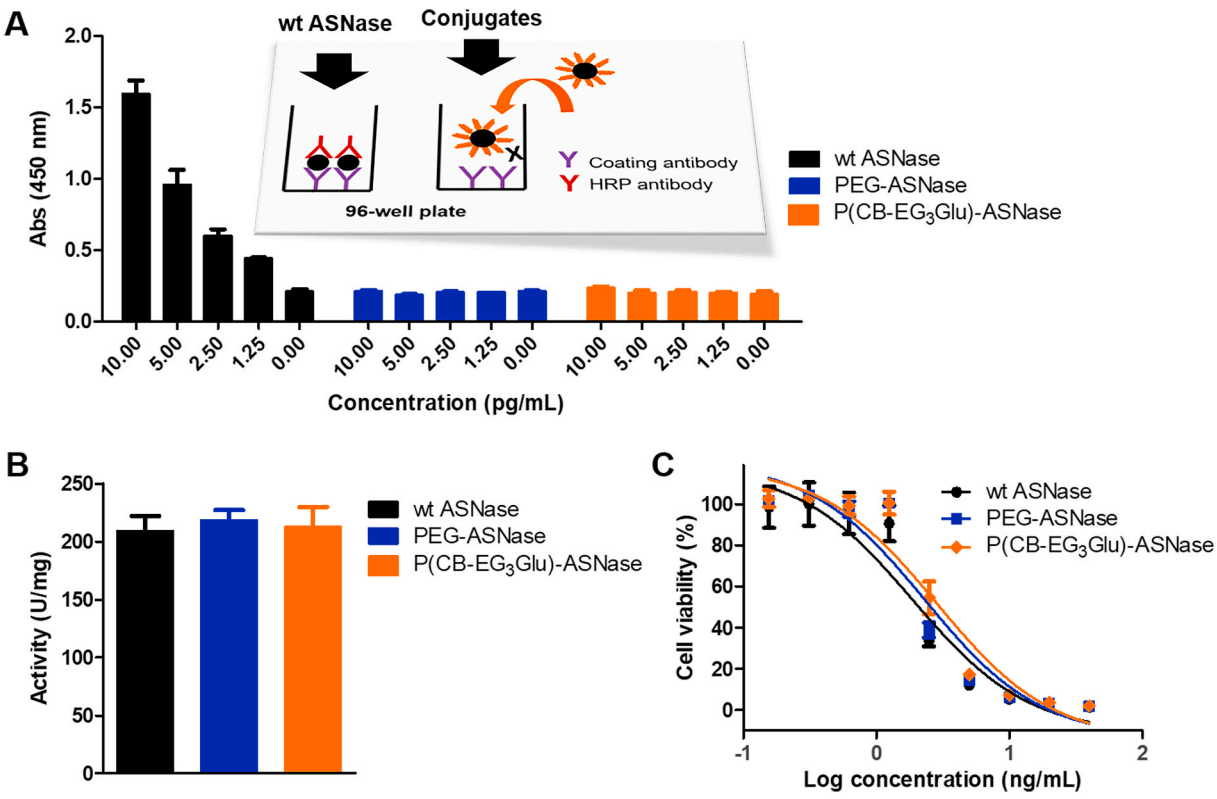

Fig. 2. In vitro epitope shielding and activity of ASNase conjugates. (A) Signals of sandwich ELISA assay detecting wt ASNase and the ASNase conjugates at gradient concentrations. Coating antibody: GTX40848 (GeneTex, USA); Detecting Antibody: ab34616 (Abcam, UK). (B) Enzymatic activity of ASNase conjugates detected using Nessler's reagent. One unit of ASNase is defined as the amount of enzyme required to generate 1 μmol of ammonia per minute at pH 7.4 and 37 °C. (C) Cytotoxicity assay. Human NKYS cell line was treated with wt ASNase or various ASNase conjugates at gradient concentrations for 48 h ($n = 3$). Data are presented as means ± standard deviations (SD). P value was determined by ANOVA, which showed significant difference between wt ASNase and conjugates (***P < 0.001) in A, while no significant difference in B and C.

of the crude mixtures (Figure S3). Conjugates in high purity were obtained after a simple size exclusion chromatography (SEC) purification, which removed the excessive polymers efficiently (Fig. 1C & S4). P(CB-EG_3Glu)-ASNase was calculated to bear approximately 20–24 polypeptide chains per ASNase tetramer by examining the intensity at both 215 and 280 nm in the UV spectroscopy (Figure S5, detailed math see SI). The two conjugates were found sharing a comparable apparent molecular weight and hydrodynamic size, as collectively demonstrated by PAGE (Fig. 1D), dynamic light scattering (DLS, Fig. 1E), and SEC (Fig. 1F). The hydrodynamic diameters of both conjugates were ~20 nm, ~12 nm greater as compared to the ~8.0 nm of the wt ASNase tetramer. Considering the theoretical length of one $_L$-P(CB-EG_3Glu)$_{40}$ chain was ~6.0 nm (0.15 nm × 40), the expected diameter of the conjugate would be ~20 nm (8.0 + 6.0 × 2, Scheme 1), agreeing well with the experimental observations. These characterizations suggested that the P(CB-EG_3Glu)-ASNase conjugate was indeed urchin-like with the polymeric "spines" forming a rigid shell (corona) of ~6 nm.

3.2. *In vitro epitope shielding and activity*

To evaluate the epitope shielding effect of the ASNase conjugates, we attempted to detect gradient concentrations of wt ASNase or ASNase conjugates in the sandwich ELISA assay using a pair of commercial anti-ASNase antibodies. Concentration-dependent signals were clearly observed for wt ASNase, validating the robustness of the assay; however, no detectable signals were found for both ASNase conjugates, indicating they had satisfactory molecular shielding characteristics under the *in vitro* condition (Fig. 2A). The *in vitro* activities of the conjugates were examined by both enzymatic and cell viability assays. The catalytic activities, measured by detecting the produced ammonium using Nessler's reagent, were almost identical for both ASNase conjugates and wt ASNase (Fig. 2B). Similarly, all of the tested ASNase variants, including wt ASNase, gave a comparable half inhibition concentration (IC_{50}) of ~2.0 ng/mL after 48 h incubation with the human NK/T lymphoma cell line NKYS (Fig. 2C). Notably, the two polymers were not toxic even at 1000 ng/mL, confirming the cytotoxicity of the conjugates were mainly derived from the enzyme ASNase (Figure S6). The unaffected biological activity of ASNase in the conjugates was remarkable, because previous studies reported 40–80% activity loss in polymersome-encapsulated ASNase [43], PEGylated ASNase using other conjugation chemistry [44], and pOEGMA-ASNase conjugates [34]. We tentatively attributed this high activity retain of our conjugates to the better substrate accessibility (as compared with ASNase-encapsulated polymersome) and/or less degree of polymer modification (~20–24 as compared with 24–36 polymer chains per ASNase tetramer for pOEGMA-ASNase conjugates).

3.3. *In vivo pharmacokinetics and pharmacodynamics*

To evaluate *in vivo* pharmacokinetics (PK), wt ASNase, P(CB-EG_3Glu)-ASNase, or PEG-ASNase was intravenously injected to SD rats at a dose of 40 U and sera were acquired at predetermined time points. Since the standard sandwich ELISA failed to determine the concentration of polymer-ASNase conjugates (Fig. 2A), the enzymatic assay described in Fig. 2B was employed to reflect the plasma concentration of ASNase based on the catalytic activity. To some extent, the functional assay may provide more precise information than common binding assays. Fortunately, analyses of the sera by using both ELISA and the enzyme activity assay gave almost identical PK profiles for wt ASNase (half-life ~1.4 h), thus validating the feasibility and accuracy of both assays for the PK purpose (Figure S7). By using the enzyme assay, the

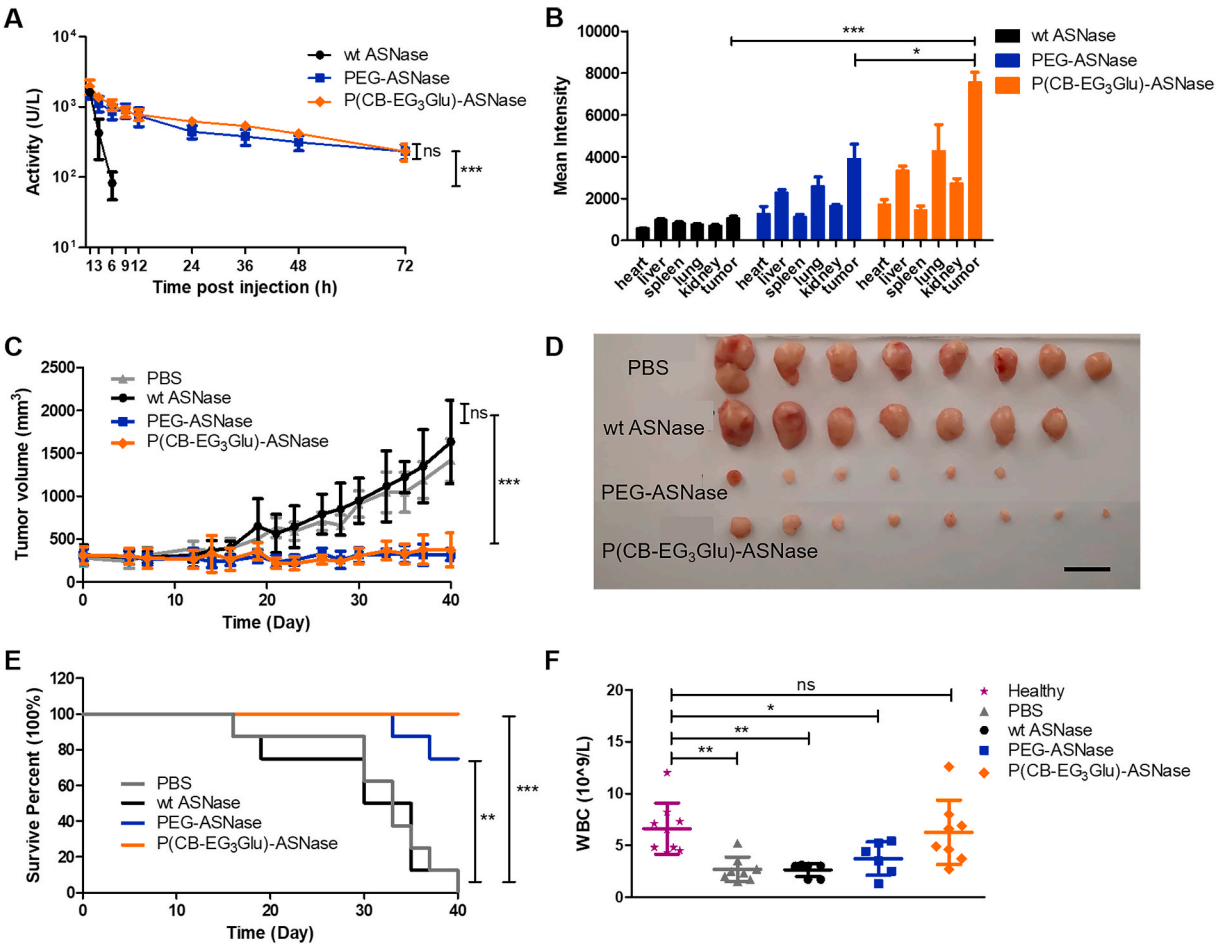

Fig. 3. In vivo pharmacological evaluation. (A) *In vivo* pharmacokinetic profiles of wt ASNase and ASNase conjugates (40 U/rat) via i.v. injection to SD rats. The enzymatic activity in plasma at various time points were measured using Nessler's reagent. (B) Mean fluorescent intensity of major organs extracted from NKYS tumor-bearing B-NDG mice that received intraperitoneal injection of Cy5-labeled wt ASNase or ASNase conjugates (20 U/mouse); animals were sacrificed 24 h post drug infusion. (C) Tumor growth curves in NKYS tumor-bearing B-NDG mice. Each mouse was s.c. inoculated 6.0×10^6 cells and tumors were allowed to grow to ~300 mm^3 before treatment; the randomized tumor-bearing mice received a biweekly intraperitoneal injection at a 15 U/mouse dose for totally three times ($n = 8$). (D) The photograph of extracted tumors on day 40; scale bar is 20 mm. (E) Survival curve. (F) White blood cell (WBC) counting on MEK-6410C (Nihon Kohden, Japan) using blood samples drawn on day 40. Data are expressed as means ± SD.

half-lives of PEG-ASNase and P(CB-EG_3Glu)-ASNase were calculated as 28.1 and 27.4 h, respectively, ~20 fold improvement compared to wt ASNase (Fig. 3A and Table S2). The AUC_{1-72h} of the two conjugates were also measured comparable (Table S2), indicating a similar level of drug exposure of these conjugates.

Next, we successfully established a NKYS tumor model in B-NDG mice, which was confirmed by immunohistochemical staining of the tumor section with a characteristic human CD56 marker (Figure S8). To explore the tumor accumulation, B-NDG mice bearing NKYS tumors were administrated with Cy5 labeled wt ASNase, PEG-ASNase or P(CB-EG_3Glu)-ASNase. 24 h post injection, mice were sacrificed and organs were extracted for the estimation of mean fluorescence intensity. Wt ASNase was found to have almost undetectable signal in all organs due to its high metabolic rate; whereas P(CB-EG_3Glu)-ASNase exhibited higher fluorescent signals in the tumor compared with PEG-ASNase (Fig. 3B and S9). In the efficacy study, when the tumors grew to ~300 mm^3 (~21 days after inoculation, day 0), the mice were randomized and received biweekly i.p. treatment of PBS, wt ASNase, PEG-ASNase, or P(CB-EG_3Glu)-ASNase at a 15 U/mouse dose ($n = 8$). On day 40, the tumor volume of all the mice in the PBS and wt ASNase groups increased to over 1000 mm^3. In contrast, treatment of both conjugates showed conspicuously better tumor growth inhibition (Fig. 3C–D), which was attributable to their substantially prolonged circulation half-lives as compared to wt ASNase. No significant loss in weight was observed for all mice in the P(CB-EG_3Glu)-ASNase group, though 2 out of 8 mice showed more than 15% weight loss for both PEG-ASNase treatment (Figure S10). As a result, at the end of the study (day 40), the survival rate was 100% (8 out of 8) for P(CB-EG_3Glu)-ASNase, and 75% (6 out of 8) for both PEG-ASNase, in sharp contrast to the 0% (0 out of 8) survival for the PBS and wt ASNase groups (Fig. 3E). The excellent biosafety profile of all ASNase variants was illustrated by the histological examination of the dissected organ sections, which showed no major damage in the heart, liver, spleen, lung, and kidney (Figure S11). Blood biochemistry analysis showed no sign of liver or kidney injury in the survived mice (Figure S12). The white blood cell (WBC) counts in PBS, wt ASNase or PEG-ASNase mice, however, were slightly but consistently lower than the healthy B-NDG mice. Interestingly, the WBC count in mice receiving P(CB-EG_3Glu)-ASNase was comparable to the averaged number in the healthy ones (Fig. 3F). The clinical implication of this phenomenon, however, needs further validation.

3.4. Immunogenicity evaluation and ABC effect

Finally, we evaluated the ADA and antipolymer antibodies in SD rats immunized with wt ASNase, PEG-ASNase, or P(CB-EG_3Glu)-ASNase weekly. Sera were acquired before the immunization (week 0), and one

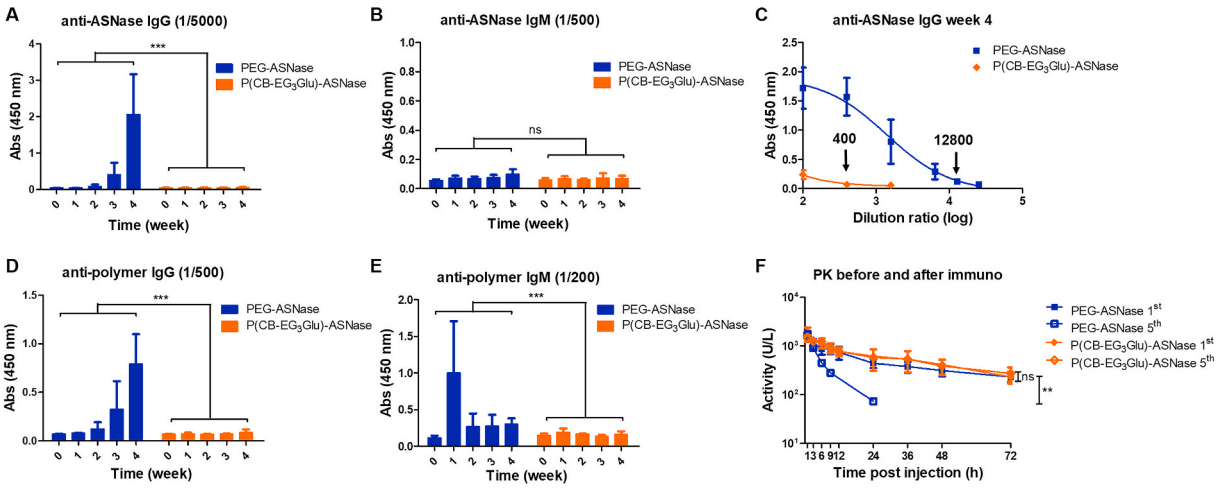

Fig. 4. In vivo antigenicity of polymer-ASNase conjugates and ABC effect evaluation. (A–B) ELISA determination of anti-ASNase IgG (A) and IgM (B) contents after each immunization. The plates were coated with wt ASNase and incubated with 5000-fold (for IgG) or 500-fold (for IgM) prediluted sera in PBS. (C) Anti-ASNase IgG levels in diluted sera drawn from the week 4. The antibody titer was defined as the maximum dilution ratio with a signal double that of blank well. (D–E) ELISA determination of anti-polymer IgG (D) and IgM (E) contents in the sera after immunization. For each polymer-of-interest, the ELISA plates were coated with the corresponding *N*-terminal specific polymer-interferon conjugate (100 μL × 1.0 μg/mL/well) and incubated with 500-fold (for IgG) or 200-fold (for IgM) prediluted sera. Immunization: SD rats were randomized ($n = 4$) and infused with wt ASNase, P(CB-EG_3Glu)-ASNase, or PEG-ASNase subcutaneously at a weekly 200 U/kg dose for 4 times. Sera were collected before the immunization (week 0), and one week after each injection but before the next dose (week 1–4). The 5th injection was performed intravenously for testing the ABC effect. ELISA condition: goat anti-rat IgG Fc HRP (ab97090) and IgM mu chain HRP (ab98373) were used as secondary antibodies; detection was based on absorption at 450 nm (A_{450}) using TMB solution (CWBIO). For anti-polymer IgG and IgM ELISA, CHAPS was used to replace Tween-20 in all buffers. (F) Pharmacokinetics of various ASNase conjugates at the 1st and 5th injections; concentration of plasma ASNase at different time points was determined by blood ASNase activity. Data are expressed as means ± SD.

week after each injection (week 1–4). As expected, immunization of wt ASNase quickly elicited both anti-ASNase IgG and IgM at substantially high levels in the sera (Figure S14). The PEG-ASNase group showed a delayed onset of the anti-ASNase IgG generation, but failed to protect the rats from immune recognition at the end of study (Fig. 4A). Remarkably, P(CB-EG_3Glu)-ASNase induced no detectable anti-ASNase IgG in the sera (Fig. 4A). No anti-ASNase IgM was detected in both groups (Fig. 4B). Analysis of the week 4 sera showed a ~30 fold greater titer of anti-ASNase IgG for the PEG-ASNase group as relative to that of P(CB-EG_3Glu)-ASNase (Fig. 4C). We further measured the antipolymer antibodies in the sera by ELISA. For PEG-ASNase, significant production of anti-PEG IgM in as early as week 2 was observed, which was later replaced by the emergence of anti-PEG IgG from week 3 (Fig. 4D–E). The specificity to PEG of the antibodies was confirmed using competition ELISA (Figure S15). A similar isotype switch was also observed previously in other PEGylated conjugates and liposomes [10,26,32,45]. On the contrary, P(CB-EG_3Glu)-ASNase were found to produce negligible anti-polymer IgG and IgM even at the end of the study (Fig. 4D–E). To examine the ABC effect, an additional i.v. injection (the 5th) was performed and the pharmacokinetic profiles were measured for both conjugates (Fig. 4F). Indeed, PEG-ASNase showed a significantly more rapid clearance from blood in the 5th drug injection as relative to the 1st injection, a clear sign of ABC effect; in contrast, P(CB-EG_3Glu)-ASNase showed no difference in drug elimination when comparing its 1st and 5th injections at the same time points.

4. Conclusion

The high immunogenicity of ASNase and PEG-ASNase can lead to loss of drug activity and/or allergic side effects, which has been a worrisome issue threatening those hypersensitive patients. More concerning, recent survey studies of healthy people have showed that more than 40% populations were tested positive in preexisting anti-PEG antibodies, a drastic surge likely due to the overwhelming use of PEG in modern society [45]. Thus, there will likely be an increasing number of patients developing HA reactions to PEGylation in the future, and the search of new alternatives to PEG becomes urgent. Zwitterionic polymers, mostly nondegradable poly(meth)acrylates-based, are outstanding antifouling materials for therapeutic protein conjugation [24–28]. Biodegradable zwitterionic polypeptides, however, are relatively less exploited for protein modification. The only exception in literation to our best knowledge is reported by Jiang and coworkers in 2018, in which an immunogenic protein uricase was studied [26]. In this work, we examined the suitability of a zwitterionic polypeptide P(CB-EG_3Glu) for ASNase modification. Different from other zwitterionic polymers, one unique feature of P(CB-EG_3Glu) is its high degree of helicity despite the high charge density along the backbone [36]. Because the substrate of ASNase is a small molecule, ~20 polymer chains can be grafted to the tetrameric enzyme without jeopardizing its catalytic activity. In the meantime, this extensive modification by the helical polypeptides forms an array of rigid "spikes" on the surface of ASNase for immune escaping. Comprehensive *in vitro* and *in vivo* evaluation revealed that both PEG-ASNase and P(CB-EG_3Glu)-ASNase: (1) shared a similarly augmented hydrodynamic size (Fig. 1), (2) retained ~100% *in vitro* activity of wt ASNase (Fig. 2), (3) prolonged the elimination half-life of ASNase for ~20 fold (Fig. 3), and (4) significantly inhibited the NKYS tumor growth in B-NDG mice (Fig. 3). Importantly, P(CB-EG_3Glu)-ASNase elicited almost no anti-ASNase/antipolymer antibodies and gave no sign of ABC effect after repetitive immunization, which is in sharp contrast compared to PEG-ASNase that developed both anti-ASNase/antipolymer antibodies and accelerated loss of ASNase activity (Fig. 4). Therefore, it is highly likely that the *in vivo* efficacy of P(CB-EG_3Glu)-ASNase would outperform PEG-ASNase in clinic or syngeneic models where patients/animals are immunocompetent. Taken together, our results demonstrate that urchin-like protein-polypeptide conjugates are outstanding candidates for reducing immunogenicity of heterologous therapeutic proteins, and P(CB-EG_3Glu)-ASNase holds great promises for various lymphoma diseases including acute lymphocytic leukemia, lymphoblastic lymphoma, and NK/T cell lymphoma.

CRediT author contribution statement

Yali Hu: Investigation, Writing - original draft. **Dedao Wang:** Investigation. **Hao Wang:** Investigation. **Ruichi Zhao:** Investigation. **Yaoyi Wang:** Investigation. **Yunfei Shi:** Resources. **Jun Zhu:** Resources, Funding acquisition. **Yan Xie:** Supervision, Funding acquisition. **Yu-Qin Song:** Supervision, Funding acquisition. **Hua Lu:** Conceptualization, Supervision, Resources, Funding acquisition, Writing - original draft.

Declaration of competing interest

The authors declare that they have no known competing financial interests or personal relationships that could have appeared to influence the work reported in this paper.

Acknowledgments

This work was supported by National Key Research and Development Program of China (2016YFA0201400), National Natural Science Foundation of China (21722401), the Clinical Medicine Plus X Young Scholars Project of Peking University (7100602769), and Capital Health Research and Development of Special (No.2018-1-2151).

Appendix A. Supplementary data

Supplementary data to this article can be found online at https://doi.org/10.1016/j.biomaterials.2020.120606.

References

[1] E. Sabattini, F. Bacci, C. Sagramoso, S.A. Pileri, WHO classification of tumours of haematopoietic and lymphoid tissues in 2008: an overview, Pathologica 102 (2010) 83–87.
[2] E. Tse, Y.-L. Kwong, The diagnosis and management of NK/T-cell lymphomas, J. Hematol. Oncol. 10 (2017) 85.
[3] W. Yong, W. Zheng, Y. Zhang, J. Zhu, Y. Wei, D. Zhu, Li, J. L-asparaginase—based regimen in the treatment of refractory midline nasal/nasal-type T/NK-cell lymphoma, Int. J. Hematol. 78 (2003) 163–167.
[4] J.M. Hill, J. Roberts, E. Loeb, A. Khan, A. MacLellan, R.W. Hill, L-asparaginase therapy for leukemia and other malignant neoplasms: remission in human leukemia, J. Am. Med. Assoc. 202 (1967) 882–888.
[5] S. Santo, J. Kapelushnik, A.M. Moser, Hypersensitivity and allergic reations to L-asparaginase in childhood ALL, Blood 110 (2007) 4331.
[6] C.T. Dellinger, T.D. Miale, Comparison of anaphylactic reactions to asparaginase derived from Escherichia coli and from Erwinia culturs, Cancer 38 (1976) 1843–1846.
[7] P.A. Dinndorf, J. Gootenberg, M.H. Cohen, P. Keegan, R. Pazdur, FDA drug approval summary: pegaspargase (Oncaspar®) for the first-line treatment of children with acute lymphoblastic leukemia (ALL), Oncol. 12 (2007) 991–998.
[8] S. Qi, J. Yahalom, M. Hsu, M. Chelius, M. Lunning, A. Moskowitz, S. Horwitz, Encouraging experience in the treatment of nasal type extra-nodal NK/T-cell lymphoma in a non-Asian population, Leuk. Lymphoma 57 (2016) 2575–2583.
[9] L.T. Henriksen, A. Harila-Saari, E. Ruud, J. Abrahamsson, K. Pruunsild, G. Vaitkeviciene, Ó.G. Jónsson, K. Schmiegelow, M. Heyman, H. Schrøder, B. K. Albertsen, PEG-asparaginase allergy in children with acute lymphoblastic leukemia in the NOPHO ALL2008 protocol, Pediatr. Blood Canc. 62 (2015) 427–433.
[10] J.K. Armstrong, G. Hempel, S. Koling, L.S. Chan, T. Fisher, H.J. Meiselman, G. Garratty, Antibody against poly(ethylene glycol) adversely affects PEG-asparaginase therapy in acute lymphoblastic leukemia patients, Cancer 110 (2007) 103–111.
[11] R.E. Rau, Z. Dreyer, M.R. Choi, W. Liang, R. Skowronski, K.P. Allamneni, M. Devidas, E.A. Raetz, P.C. Adamson, S.M. Blaney, M.L. Loh, S.P. Hunger, Outcome of pediatric patients with acute lymphoblastic leukemia/lymphoblastic lymphoma with hypersensitivity to pegaspargase treated with PEGylated Erwinia asparaginase, pegcrisantaspase: a report from the Children's Oncology Group, Pediatr. Blood Canc. 65 (2018), e26873.
[12] E.M. Pelegri-O'Day, E.-W. Lin, H.D. Maynard, Therapeutic protein–polymer conjugates: advancing beyond PEGylation, J. Am. Chem. Soc. 136 (2014) 14323–14332.
[13] K. Knop, R. Hoogenboom, D. Fischer, U.S. Schubert, Poly(ethylene glycol) in drug delivery: pros and cons as well as potential alternatives, Angew. Chem. Int. Ed. 49 (2010) 6288–6308.
[14] I. Ekladious, Y.L. Colson, M.W. Grinstaff, Polymer–drug conjugate therapeutics: advances, insights and prospects, Nat. Rev. Drug Discov. 18 (2019) 273–294.
[15] J. Kopeček, Polymer–drug conjugates: origins, progress to date and future directions, Adv. Drug Deliv. Rev. 65 (2013) 49–59.
[16] C. Chen, D.Y.W. Ng, T. Weil, Polymer bioconjugates: modern design concepts toward precision hybrid materials, Prog. Polym. Sci. 105 (2020) 101241.
[17] P. Wilson, J. Nicolas, D.M. Haddleton, Polymer–protein/peptide bioconjugates (Chapter 12), in: Chemistry of Organo-Hybrids, 2015, pp. 466–502.
[18] V. Schellenberger, C.-w. Wang, N.C. Geething, B.J. Spink, A. Campbell, W. To, M. D. Scholle, Y. Yin, Y. Yao, O. Bogin, J.L. Cleland, J. Silverman, W.P.C. Stemmer, A recombinant polypeptide extends the in vivo half-life of peptides and proteins in a tunable manner, Nat. Nanotechnol. 27 (2009) 1186–1190.
[19] U. Binder, A. PASylation® Skerra, A versatile technology to extend drug delivery, Curr. Opin. Colloid In 31 (2017) 10–17.
[20] J. Hu, G. Wang, X. Liu, W. Gao, Enhancing pharmacokinetics, tumor accumulation, and antitumor efficacy by elastin-like polypeptide fusion of interferon alpha, Adv. Mater. 27 (2015) 7320–7324.
[21] F. Wurm, C. Dingels, H. Frey, H.-A. Klok, Squaric acid mediated synthesis and biological activity of a library of linear and hyperbranched poly(glycerol)–protein conjugates, Biomacromolecules 13 (2012) 1161–1171.
[22] M. Ferraro, K. Silberreis, E. Mohammadifar, F. Neumann, J. Dernedde, R. Haag, Biodegradable polyglycerol sulfates exhibit promising features for anti-inflammatory applications, Biomacromolecules 19 (2018) 4524–4533.
[23] A. Mero, Z. Fang, G. Pasut, F.M. Veronese, T.X. Viegas, Selective conjugation of poly(2-ethyl 2-oxazoline) to granulocyte colony stimulating factor, J. Contr. Release 159 (2012) 353–361.
[24] S. Yan, C. Zhang, H. Lu, Advances in zwitterionic polymers, J. Funct. Polym. 33 (2020) 1–14.
[25] X. Han, Y. Lu, J. Xie, E. Zhang, H. Zhu, H. Du, K. Wang, B. Song, C. Yang, Y. Shi, Z. Cao, Zwitterionic micelles efficiently deliver oral insulin without opening tight junctions, Nat. Nanotechnol. 15 (2020) 605–614.
[26] P. Zhang, P. Jain, C. Tsao, Z. Yuan, W. Li, B. Li, K. Wu, H.-C. Hung, X. Lin, S. Jiang, Polypeptides with high zwitterion density for safe and effective therapeutics, Angew. Chem. Int. Ed. 57 (2018) 7743–7747.
[27] S. Liang, Y. Liu, X. Jin, G. Liu, J. Wen, L. Zhang, J. Li, X. Yuan, I.S.Y. Chen, W. Chen, H. Wang, L. Shi, X. Zhu, Y. Lu, Phosphorylcholine polymer nanocapsules prolong the circulation time and reduce the immunogenicity of therapeutic proteins, Nano Research 9 (2016) 1022–1031.
[28] A.J. Keefe, S. Jiang, Poly(zwitterionic)protein conjugates offer increased stability without sacrificing binding affinity or bioactivity, Nat. Chem. 4 (2011) 59–63.
[29] C. Fu, B. Demir, S. Alcantara, V. Kumar, F. Han, H.G. Kelly, X. Tan, Y. Yu, W. Xu, J. Zhao, C. Zhang, H. Peng, C. Boyer, T.M. Woodruff, S.J. Kent, D.J. Searles, A. K. Whittaker, Low-fouling fluoropolymers for bioconjugation and InVivo tracking, Angew. Chem. Int. Ed. 59 (2020) 4729–4735.
[30] Z.-H. Peng, J. Kopeček, HPMA copolymer CXCR4 antagonist conjugates substantially inhibited the migration of prostate cancer cells, ACS Macro Lett. 3 (2014) 1240–1243.
[31] O. Zagorodko, J.J. Arroyo-Crespo, V.J. Nebot, M.J. Vicent, Polypeptide-based conjugates as therapeutics: opportunities and challenges, Macromol. Biosci. 17 (2017), 1600316.
[32] Y. Hu, Y. Hou, H. Wang, H. Lu, Polysarcosine as an alternative to PEG for therapeutic protein conjugation, Bioconjugate Chem. 29 (2018) 2232–2238.
[33] P. Caliceti, O. Schiavon, F.M. Veronese, Immunological properties of uricase conjugated to neutral soluble polymers, Bioconjugate Chem. 12 (2001) 515–522.
[34] M. Liu, P. Johansen, F. Zabel, J.-C. Leroux, M.A. Gauthier, Semi-permeable coatings fabricated from comb-polymers efficiently protect proteins in vivo, Nat. Commun. 5 (2014) 5526.
[35] Y. Qi, A. Simakova, N.J. Ganson, X. Li, K.M. Luginbuhl, I. Ozer, W. Liu, M. S. Hershfield, K. Matyjaszewski, A. Chilkoti, A brush-polymer/exendin-4 conjugate reduces blood glucose levels for up to five days and eliminates poly(ethylene glycol) antigenicity, Nat. Biomed. Eng. 1 (2016), 0002.
[36] C. Zhang, J. Yuan, J. Lu, Y. Hou, W. Xiong, H. Lu, From neutral to zwitterionic poly (α-amino acid) nonfouling surfaces: effects of helical conformation and anchoring orientation, Biomaterials 178 (2018) 728–737.
[37] C. Zhang, H. Lu, Efficient synthesis and application of protein-poly(α-amino acid) conjugates, Acta Polym. Sin. 1 (2018) 21–31.
[38] Y. Hou, Y. Zhou, H. Wang, J. Sun, R. Wang, K. Sheng, J. Yuan, Y. Hu, Y. Chao, Z. Liu, H. Lu, Therapeutic protein PEPylation: the helix of nonfouling synthetic polypeptides minimizes antidrug antibody generation, ACS Cent. Sci. 5 (2019) 229–236.
[39] Z. Yuan, B. Li, L. Niu, C. Tang, P. McMullen, P. Jain, Y. He, S. Jiang, Zwitterionic peptide cloak mimics protein surfaces for protein protection, Angew. Chem. Int. Ed. 59 (2020) 22378–22381.
[40] Y.Q. Hou, J.S. Yuan, Y. Zhou, J. Yu, H. Lu, A concise approach to site-specific topological protein-poly(amino acid) conjugates enabled by in situ-generated functionalities, J. Am. Chem. Soc. 138 (2016) 10995–11000.
[41] A.L. Swain, M. Jaskólski, D. Housset, J.K. Rao, A. Wlodawer, Crystal structure of Escherichia coli L-asparaginase, an enzyme used in cancer therapy, Proc. Natl. Acad. Sci. Unit. States Am. 90 (1993) 1474.
[42] C. Zhang, J. Lu, Y. Hou, W. Xiong, K. Sheng, H. Lu, Investigation on the linker length of synthetic zwitterionic polypeptides for improved nonfouling surfaces, ACS Appl. Mater. Interfaces 10 (2018) 17463–17470.
[43] L.D. Blackman, S. Varlas, M.C. Arno, Z.H. Houston, N.L. Fletcher, K.J. Thurecht, M. Hasan, M.I. Gibson, R.K. O'Reilly, Confinement of therapeutic enzymes in selectively permeable polymer vesicles by polymerization-induced self-assembly

(PISA) reduces antibody binding and proteolytic susceptibility, ACS Cent. Sci. 4 (2018) 718–723.
[44] G.P. Meneguetti, J.H.P.M. Santos, K.M.T. Obreque, C.M.V. Barbosa, G. Monteiro, S. H.P. Farsky, A. Marim de Oliveira, C.B. Angeli, G. Palmisano, S.P.M. Ventura, A. Pessoa-Junior, C. de Oliveira Rangel-Yagui, Novel site-specific PEGylated L-asparaginase, PloS One 14 (2019) e0211951.
[45] P. Zhang, F. Sun, S. Liu, S. Jiang, Anti-PEG antibodies in the clinic: current issues and beyond PEGylation, J. Contr. Release 244 (2016) 184–193.